Spatially resolved spectroscopy on superconducting proximity nanostructures

M. Vinet, C. Chapelier, and F. Lefloch
Département de Recherche Fondamentale sur la Matière Condensée, SPSMS, CEA-Grenoble, 17 rue des Martyrs, 38054 Grenoble Cedex 9, France

(Received 2 October 2000; published 4 April 2001)

We investigated the local density of states (LDOS) of a normal metal (N) in good electrical contact with a superconductor (S) as a function of the distance x to the NS interface. The sample consists of a pattern of alternate strips of Au and Nb. We used a low-temperature scanning tunneling microscope to record simultaneously $dI/dV(V,x)$ curves and the topographic profile $z(x)$. Nearby the NS interface, all the spectra show a dip at the Fermi energy but, depending on the geometry, different behaviors can be distinguished. First, when the characteristic size of the normal metal L is much larger than the coherence length $\xi_N=\sqrt{\hbar D_N/2\Delta}$, the spectral extension of the dip decreases from Δ at the NS interface to zero at distances $x\gg\xi_N$. Second, when L is comparable to ξ_N, the apparent gap in the LDOS is space independent.

DOI: 10.1103/PhysRevB.63.165420 PACS number(s): 74.50.+r, 73.40.Gk, 73.50.Bk

A normal metal (N) in good metallic contact with a superconductor (S) can acquire some superconducting properties and reciprocally the superconductivity can be affected by the normal metal vicinity. This proximity effect has been first extensively studied in the late 1960s using the Ginzburg-Landau theory which describes macroscopic superconducting systems near their transition temperature T_c.[1,2] Recent advances in nanofabrication renewed the interest in this phenomenon, especially at the mesoscopic scale when the characteristic size L of the normal metal becomes smaller than the thermal length $L_T=\sqrt{\hbar D_N/2\pi k_B T}$ (D_N is the diffusion constant in the normal metal). Simultaneously a more comprehensive understanding of the proximity effect in the diffusive regime based on the theory of nonequilibrium superconductivity has emerged.[3,4] The predictions made on the local density of states (LDOS) in N depend on the ratio L/ξ_N, where L is the size of the normal metal and $\xi_N=\sqrt{\hbar D_N/2\Delta}$ its coherence length (Δ is the superconducting gap).[4] On the one hand, when $L\gg\xi_N$ (infinite system), the superconducting correlations induced in N lead to a depression of the electronic density of states around the Fermi energy E_F. The energy scale of this dip in the LDOS vanishes to zero at increasing distances from the NS interface. On the other hand, when L is comparable to ξ_N (finite system) the LDOS shows a space independent minigap E_g whose width is related to the Thouless energy $E_{Th}=\hbar D/L^2$. However, when $L\leqslant l_N$ (l_N is the elastic mean free path in N), E_g goes like L/l_N and eventually vanishes in the pure ballistic case.[5]

Experimental tests of the theory in the infinite case were obtained by Guéron *et al.*[6] They used nanofabricated tunnel junctions to measure the electronic density of states $n(E,x)$ at three distinct positions along a normal wire in contact with a superconductor. However, because of the size of these junctions they could not achieve a spatial resolution better than ξ_N and the closest spot probed was at about two ξ_N from the NS interface. On a much smaller scale, scanning tunneling microscopy (STM) was used to study the proximity effect in ballistic N metals (i.e., $L\ll\xi_N,l_N$).[7,8] In these experiments the LDOS crucially depends on the thickness of the normal system. The shape of the spectra is explained within the de Gennes–Saint James bound-states model.[9] Other STM experiments on small N wires embedded in an S matrix showed a healing length of superconductivity on the S side much larger than the coherence length ξ_S.[10] But according to the authors, they could not easily interpret the spatial dependence of the LDOS in the N metal because of a complicated geometry.

We report here measurements of the local electronic density of states by scanning tunneling spectroscopy on Nb/Au proximity junctions. Since STM allows a high energetic and spatial resolution in conjunction with sample topography, we are able to spatially resolve the LDOS in the normal metal as a function of the distance x to the NS interface (x can vary from zero to several coherence lengths with a resolution of a few nanometers). Moreover, we can discriminate between the two situations: $L\leqslant\xi_N$ and $L\gg\xi_N$ within the same sample.

Our STM hangs inside a sealed tube by a 1-m-long spring to decouple it from external vibrations. This tube is immersed in a He^4 cryostat and cooling is achieved by introducing high purity helium exchange gas into the tube. The temperature is then reduced to 1.5 K by pumping on the helium bath. Tunneling spectra are obtained by a lock-in detection technique with a 77-μV peak-to-peak modulation voltage of the bias at 1 kHz. We measure the differential conductance dI/dV versus V while holding the STM tip at a fixed height above each position $\mathbf{r}$. This provides a local probe of the LDOS $n(eV,\mathbf{r})$. The energetic resolution is determined by the thermal broadening at 1.5 K. Each curve is a single acquisition process with no additional averaging. The dI/dV curves and the topography are measured during the same line scan allowing us to correlate them precisely. Data are normalized to the conductance at high voltage ($V>\Delta$). The *same* normalization coefficient has been used for all the curves. The typical tunneling resistance is $10^7\Omega$.

We have chosen Au as a normal metal because it is chemically inert. The Au film has been previously characterized by measuring the temperature dependence of the resistivity, $R(T)$, which gives a mean free path $l_N\simeq 22$ nm and a diffusion coefficient $D_N\simeq 1.0\times 10^{-2}$ $m^2\,s^{-1}$ leading to $\xi_N\simeq 53$ nm. Nb is used as a superconductor because of its high

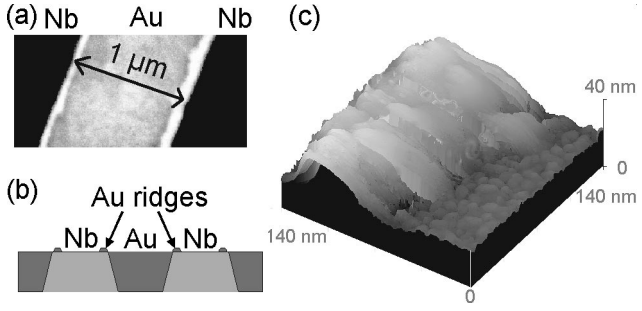

FIG. 1. (a) Scanning electron microscope photography of the sample displaying the small ridges on each side of the Au strip. (b) Schematic cross section of the sample. It consists of a 50-nm-thick pattern of self-aligned strips 1 μm wide and 250 μm long of Au and Nb. (c) A $140\times140\times40$ nm^3 topographic STM picture of a Au ridge.

critical temperature. Our 50-nm-thick Nb film undergoes a BCS transition at 8.1 K and shows an energy gap $\Delta \simeq 1.15$ meV at 1.5 K. Its coherence length is $\xi_S = \sqrt{\hbar D_S/2\Delta} \simeq 27$ nm and the mean free path is $l_S \simeq 6$ nm given by $R(T)$ measurements. The ratio $l_S/\xi_S < 1$ is characteristic of a dirty superconductor.

Our sample consists of a 50-nm-thick pattern of juxtaposed strips, 1 μm wide and 250 μm long, of Au and Nb in good electrical contact, see Figs. 1(a) and 1(b). The Nb was first uniformly deposited by dc sputtering on a thermally oxidized Si wafer. We used uv lithography and subsequent reactive ion etching (RIE) to produce the Nb strips. 10% of oxygen was introduced in the SF_6 plasma during RIE in order to remove all organic residues and to give some inclination to the edges of the Nb strips [see Fig. 1(b) where this inclination has been quite exaggerated]. This ensures a *NS* interface over the full height of the layers. We then sputtered 2-nm Ti and 50-nm Au to fill up the grooves between the Nb strips and lifted-off the remaining resist. Prior to the Ti/Au sputtering the Nb surface has been cleaned and the native oxide removed by an *in situ* inverse plasma shallow etching to ensure a good metallic contact. As seen in Figs. 1(a) and 1(c), Au forms ridges on each side of the Nb strips. The size of these ridges has been measured both by STM and scanning electron microscopy. Their lateral dimensions vary from 50 to 200 nm and their heights from 10 to 50 nm. They are in electrical contact with Nb but poorly connected to the rest of Au. Indeed we observe BCS-like $dI/dV(V)$ curves in between the Au ridges and the Au strips which indicates the presence of bare Nb (see the lower curve of Fig. 2). The solid line represents the convolution of the BCS density of states with a Fermi-Dirac distribution at the measured temperature $T = 1.5$ K. We introduce a phenomenological parameter Γ to define a complex energy $E^* = E - i\Gamma$.[11] This parameter reflects the broadening of the energy levels due to the finite lifetime of the quasiparticles. The calculation provides a superconducting gap $\Delta = 1.15$ meV and $\Gamma = 0.07\Delta$. In contrast spectra taken above Au either over the ridges or the strips cannot be fitted using this model. As an illustration, the upper part of Fig. 2 shows calculated curves with different sets of the parameters Δ and Γ. The transition from these two types of spectra allows us to infer the *NS* interface.

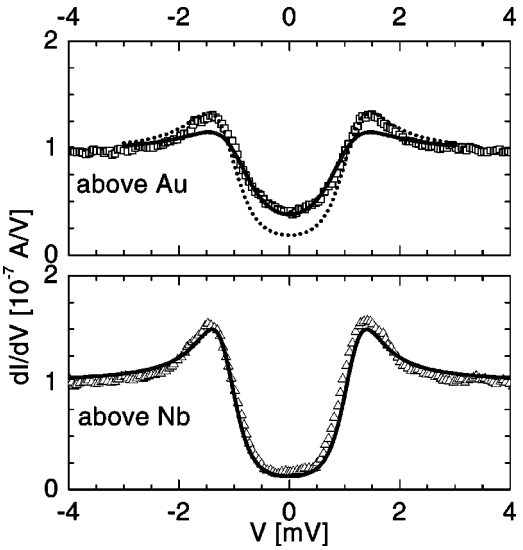

FIG. 2. Two spectra taken above either Au or Nb. Above the Nb film (lower curve) the spectrum is fitted within a BCS model with $\Delta = 1.15$ meV and $\Gamma = 0.07\Delta$ (solid line). In contrast this model cannot describe simultaneously the wings and the zero-bias conductance of the spectra taken above Au (upper curve). The dotted line is a fit with $\Delta = 1.1$ meV, $\Gamma = 0.12\Delta$ whereas the solid one is for $\Delta = 1.1$ meV, $\Gamma = 0.40\Delta$.

In order to describe our results we need to take into account the coherence effects of the quasiparticles inside the normal metal. In the framework of the quasiclassical Green's function formalism, induced correlations between electrons of opposite spin in the normal metal are described by a complex angle $\theta(E,\mathbf{r})$.[4,12] The LDOS of the quasiparticles n is related to θ by $n(E,\mathbf{r}) = n_0\,\mathrm{Re}[\cos\theta(E,\mathbf{r})]$. In the dirty limit and in zero magnetic field, $\theta(E,\mathbf{r})$ obeys the one-dimensional (1D) diffusion Usadel equation:[13]

$$\frac{\hbar D}{2}\frac{\partial^2\theta}{\partial x^2} + [iE - \Gamma_{in} - 2\Gamma_{sf}\cos\theta]\sin\theta + \Delta(x)\cos\theta = 0, \tag{1}$$

where Γ_{sf} and Γ_{in} are the spin-flip and the inelastic scattering rates, respectively, and $\Delta(x)$ is the pair potential. The order parameter is space dependent and obeys a self-consistent equation.[3,4] However, for the sake of simplicity we assume no pair potential in the normal metal ($\Delta_N = 0$) whereas we take Δ equals to its bulk value everywhere in the superconductor. Conditions of continuity, $\theta_{x=0^-} = \theta_{x=0^+}$, and spectral current conservation $\sigma_S(\partial\theta/\partial x)_{x=0^-} = \sigma_N(\partial\theta/\partial x)_{x=0^+}$ are imposed at the *NS* interface which is valid in the case of a perfect electrical contact. This assumption is justified by the careful cleaning of the Nb surface prior to the normal films deposition. However, the presence of Ti and the possible alloying of the different metals complicates a lot of the actual interface description. We therefore choose to introduce an effective conductivity σ_{Neff} instead of the gold one σ_N.

When $L \gg \xi_N$, the normal metal can be considered as semi-infinite and one recovers the N density of states far away from the superconductor. The boundary condition of

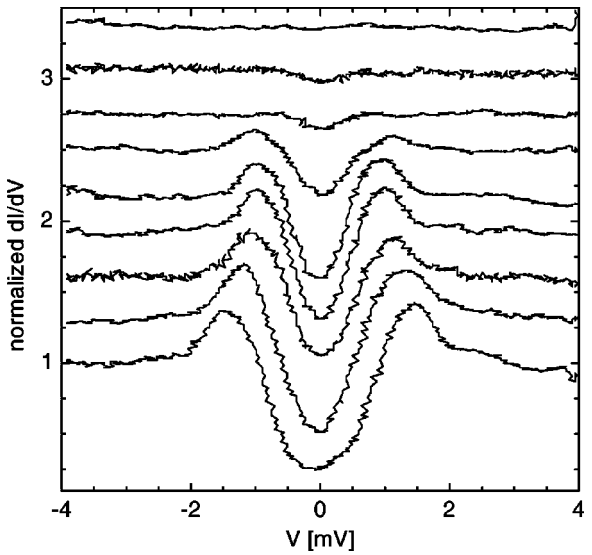

FIG. 3. Spectra taken at different positions above the wide strip of Au. The curves have been evenly shifted for clarity. The pseudogap decreases from Δ at the *NS* interface (lower curve) to 0 at distances larger than 220 nm (upper curve).

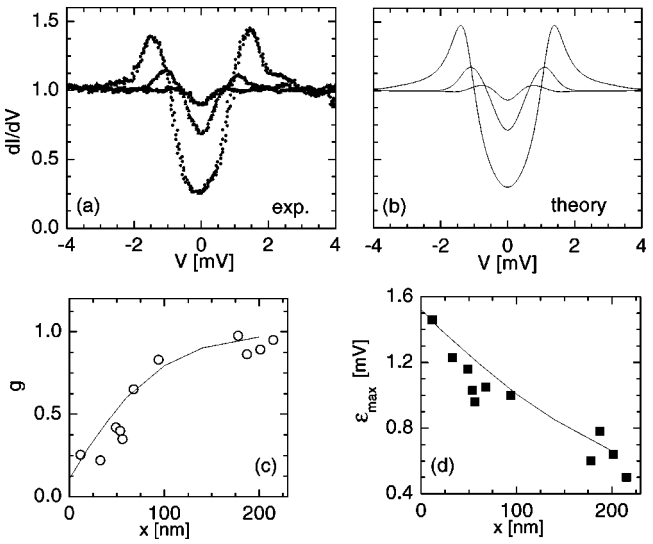

FIG. 4. (a) Measured spectra at 20, 75, and 195 nm from the interface. (b) Calculated spectra at 20, 80, and 160 nm. (c) and (d) represent, respectively, the normalized zero-bias conductance g and the energy of the peak ε_{max}, as a function of the distance x to the *NS* interface. The solid lines correspond to the fit.

Eq. (1) on the *N* side is then $\theta(E,\infty)=\theta_N=0$. This situation corresponds to the 1-μm-wide strip of Au. In the first set of experiments we scanned above its surface and measured the LDOS as a function of the distance x to the *NS* interface, located within ± 5 nm. The spectra were taken along the same line perpendicular to the interface. The space-dependent LDOS is plotted in Fig. 3 for different x. Because of the uncertainty about piezoelectric coefficients of the scanning tube at low temperature, we estimate an accuracy on x of the order of 20%.

We observe a peak in $G_V(x)=dI/dV(V,x)$ at an energy ε_{max} which decreases as we move away from the superconductor. Figure 4(d) displays ε_{max} (solid squares) and Fig. 4(c) the normalized zero-bias conductance $g=G_{V=0}/G_{V=4\ \mathrm{mV}}$ (open circles) as a function of x. A zero density of states at the Fermi level is never observed due to pair-breaking mechanisms such as spin-flip and inelastic scattering that cannot be neglected at 1.5 K. The fluctuations of g and ε_{max} are not due to experimental noise but are correlated to changes in the Au-film morphology related to different grains. A slight dispersion of the properties of these grains may explain such nonmonotic evolutions.[8] We compare our measurements to the convolution of the LDOS calculated from Eq. (1) with a Fermi-Dirac distribution. For the superconducting part, we used the value of Δ and Γ_{in} given by the BCS fit above Nb. For the normal part, the rates Γ_{in}, Γ_{sf}, the coherence length ξ_N, and the ratio σ_S/σ_{Neff} are taken as adjustable parameters. The solid lines in Figs. 4(c) and 4(d) represent, respectively, the computed values of g and ε_{max}. As can be seen in Figs. 4(a) and 4(b), the experimental spectra obtained at distances $x=20$, 75, and 195 nm are very similar to the calculated ones at distances 20, 80, and 160 nm with $\sigma_S/\sigma_{Neff}=4$ and $\xi_N=70$ nm. This latter value is slightly bigger than the coherence length evaluated from the conductance of the bulk film. This discrepancy might be due either to local fluctuations of D_N or to the crude 1D approximation of the theoretical model. Nevertheless it reproduces well both the shapes of the spectra and their spatial evolution. Moreover, the fits are sensitive in different ways to the two scattering rates. However, this difference is blurred by the temperature and we cannot exclude a possible mixture of the two mechanisms from our calculations. Yet we are able to deduce a spin-flip time $\tau_{sf}=\hbar/\Gamma_{sf}=4$ ps in good agreement with recent experiments.[14]

In the second step of experiments, we have investigated the LDOS over two small ridges of Au. They are lying over Nb and the *NS* interface is now horizontal. Due to the initial slope of their edges, when moving the STM tip horizontally we can change the distance to the *NS* interface (see the inset

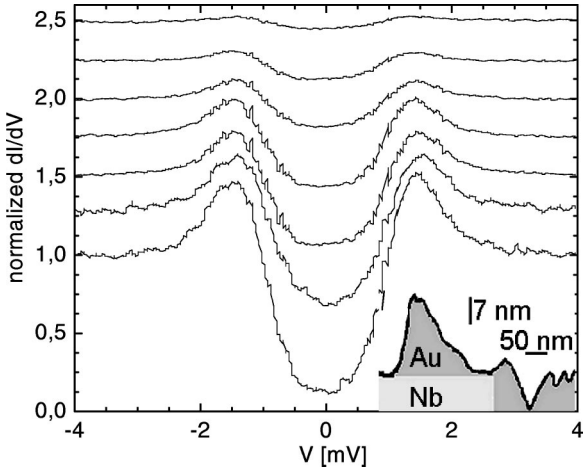

FIG. 5. Spectra taken at different positions above a ridge 20 nm high. The curves have been evenly shifted for clarity. The lower curve has been taken at the bottom of the ridge and the upper one at the top of it. The inset is a STM profile of the ridge.

of Fig. 5). Similarly to the work of Tessmer *et al.*[7] but unlike experiments where the proximity effect was probed on *NS* bilayers with different thicknesses,[8] we do not change the overall size of the normal system between different spectra but only the distance to the *NS* interface. Therefore we obtain the actual spatial dependence of the LDOS $n(E,x)$ of a normal system with a fixed dimension L.

In this configuration we find that the position of the peaks in $dI/dV(V,x)$ does not depend on the distance to the *NS* interface in striking contrast to the preceding case (see Fig. 5). For a ridge of 20-nm height, we observe that the maximum is located at 1.5 meV whereas in a ridge of height 50 nm, the position of the peak is 0.95 meV. Theoretically, in a finite diffusive geometry, i.e., when $L \simeq \xi_N \gg l_N$, the N side boundary condition of Eq. (1) is $(\partial\theta/\partial x)(E,x=L)=0$ and a minigap E_g is predicted to appear in the LDOS.[4] E_g is related to the Thouless energy $E_{Th}=\hbar D_N/L^2$ through $E_g = \Delta(1+L/2.1\xi_N)^{-2}$. In the small ridge, $E_{Th}=18$ meV$\gg\Delta$, the minigap is limited by the superconducting one. On the contrary, in the bigger ridge, $E_{Th}=2.8$ meV that yields to a minigap $E_g=0.53$ meV. Although we measure the position of the peaks and not E_g, our results are consistent with a size-dependent minigap. However, because of the uncontrolled fabrication of the Au ridges fluctuations of the *NS* interface transparency might also affect the value of E_g.

In conclusion, we have probed the proximity effect in two different systems. First, we have investigated the LDOS of a semi-infinite normal metal and found space-dependent energy spectra as a function of the distance to the *NS* interface. This behavior is qualitatively and quantitatively in very good agreement with the pseudogap model predicted by the theory of nonequilibrium superconductivity. We have also investigated the local density of states in a confined geometry. In this case we have found a spectral structure that does not vary in space and which can be related to the Thouless energy.

We wish to acknowledge beneficial discussions with M. Sanquer and the valuable help of J. C. Toussaint for numerical calculations.

[1] G. Deutscher and P. G. de Gennes, in *Superconductivity*, edited by R. D. Parks (Dekker, New York, 1969), p. 1005.
[2] E. L. Wolf and G. B. Arnold, Phys. Rep. **91**, 31 (1982).
[3] C. Bruder, Supercond. Rev. **1**, 261 (1996); A. F. Volkov, A. V. Zaitsev, and T. M. Klapwijk, Physica C **210**, 21 (1993); A. A. Golubov, F. K. Wilhelm, and A. D. Zaïkin, Phys. Rev. B **55**, 1123 (1997).
[4] W. Belzig, C. Bruder, and Gerd Schön, Phys. Rev. B **54**, 9443 (1996).
[5] S. Pilgram, W. Belzig, and C. Bruder, Physica B **280**, 442 (2000).
[6] S. Guéron, H. Pothier, Norman O. Birge, D. Estève, and M. H. Devoret, Phys. Rev. Lett. **77**, 3025 (1996).
[7] S. H. Tessmer, D. J. Van Harlingen, and J. W. Lyding, Phys. Rev. Lett. **70**, 3135 (1993); S. H. Tessmer, M. B. Tarlie, D. J. Van Harlingen, D. L. Maslov, and P. M. Goldbart, *ibid.* **77**, 924 (1996).
[8] A. D. Truscott, R. C. Dynes, and L. F. Schneemeyer, Phys. Rev. Lett. **83**, 1014 (1999).
[9] P. G. de Gennes and D. Saint-James, Phys. Lett. **4**, 151 (1963).
[10] Y. Levi, O. Millo, N. D. Rizzo, D. E. Prober, and L. R. Motowidlo, Phys. Rev. B **58**, 15 128 (1998).
[11] R. C. Dynes, V. Narayanamurti, and J. P. Garno, Phys. Rev. Lett. **41**, 1509 (1978).
[12] D. Estève, H. Potier, S. Guéron, Norman O. Birge, and M. Devoret, in *Correlated Fermions and Transport in Mesoscopic Systems*, edited by T. Martin *et al.* (Éditions Frontières, Paris, 1996), p. 297.
[13] K. D. Usadel, Phys. Rev. Lett. **25**, 507 (1970).
[14] A. B. Gougam, F. Pierre, H. Pothier, D. Estève, and N. O. Birge, J. Low Temp. Phys. **118**, 447 (2000).